CFSTI PRICES

H.C. $3.00 ; MN 65

ORNL-TM-1692

Contract No. W-7405-eng-26

METALS AND CERAMICS DIVISION

RELEASED FOR ANNOUNCEMENT

IN NUCLEAR SCIENCE ABSTRACTS

CHARACTERIZATION OF U_3O_8 DISPERSIONS IN ALUMINUM

D. O. Hobson C. F. Leitten, Jr.

LEGAL NOTICE

This report was prepared as an account of Government sponsored work. Neither the United States, nor the Commission, nor any person acting on behalf of the Commission:

A. Makes any warranty or representation, expressed or implied, with respect to the accuracy, completeness, or usefulness of the information contained in this report, or that the use of any information, apparatus, method, or process disclosed in this report may not infringe privately owned rights; or

B. Assumes any liabilities with respect to the use of, or for damages resulting from the use of any information, apparatus, method, or process disclosed in this report.

As used in the above, "person acting on behalf of the Commission" includes any employee or contractor of the Commission, or employee of such contractor, to the extent that such employee or contractor of the Commission, or employee of such contractor prepares, disseminates, or provides access to, any information pursuant to his employment or contract with the Commission, or his employment with such contractor.

FEBRUARY 1967

OAK RIDGE NATIONAL LABORATORY
OAK RIDGE, TENNESSEE
operated by
UNION CARBIDE CORPORATION
for the
U.S. ATOMIC ENERGY COMMISSION

DISCLAIMER

This report was prepared as an account of work sponsored by an agency of the United States Government. Neither the United States Government nor any agency Thereof, nor any of their employees, makes any warranty, express or implied, or assumes any legal liability or responsibility for the accuracy, completeness, or usefulness of any information, apparatus, product, or process disclosed, or represents that its use would not infringe privately owned rights. Reference herein to any specific commercial product, process, or service by trade name, trademark, manufacturer, or otherwise does not necessarily constitute or imply its endorsement, recommendation, or favoring by the United States Government or any agency thereof. The views and opinions of authors expressed herein do not necessarily state or reflect those of the United States Government or any agency thereof.

DISCLAIMER

Portions of this document may be illegible in electronic image products. Images are produced from the best available original document.

CONTENTS

CHARACTERIZATION OF U_3O_8 DISPERSIONS IN ALUMINUM

D. O. Hobson C. F. Leitten, Jr.

ABSTRACT

Characterization of dispersion fuels is essential for establishing material and process specifications and can help predict irradiation performance. The highly fragmented and stringered nature of oxides in fabricated aluminum-base dispersions required the development of an improved technique to quantitatively evaluate dispersions containing nonspherical dispersoids. In place of using the point or line methods developed for spherical oxides, a fragmentation ratio was measured by counting the small fragments generated from the original particles during fabrication. This technique was successfully demonstrated by evaluating the propensity of three different commercial grades of U_3O_8 powder to fragment and stringer during plate fabrication. The resistance of the oxide to fragmentation and stringering varied with oxide density, particle sphericity, surface area, and particle spacing. Generally, the fragmentation ratio decreased with increasing particle density and sphericity. Fuel inhomogeneity also induced particle fragmentation. Stringering increased with increasing oxide surface area but depended strongly on processing and the ability of the oxide to resist fragmentation.

INTRODUCTION

The operating parameters of advanced research reactors have imposed severe requirements on the performance and reliability of aluminum-base fuels. Unlike the now conventional test reactors, the higher thermal and neutron fluxes of the advanced reactors dictate rigid control of fuel content and homogeneity within the plates. Such tolerances are difficult to achieve with conventional uranium alloy technology. Dispersions, however, afford the advantages of accurate total fuel loading, ability to incorporate controlled known amounts of a burnable poison, and fabricability with higher fuel concentrations. Although considerable work has been done in developing the fabrication technology for aluminum-base dispersions, only limited studies have been made to characterize the dispersions.

Characterization of a fuel dispersion is desirable for at least two purposes. The first of these is to develop a method to predict the irradiation behavior of a fuel plate from a knowledge of the reaction of the fuel to the fabrication procedures. The second is to characterize the fabrication behavior of the fuel so that one can know what properties to specify when purchasing commercial fuel. We believe that an evaluation of the fragmentation and stringering properties of U_3O_8 dispersed in aluminum, based on criteria such as oxide density, surface area, and fabrication procedures, can provide data that, when combined with results of irradiation testing, will afford a sound basis for predicting irradiation behavior.

Various characterization methods for the evaluation of fuel dispersions have been developed in the past. Generally, these were of little use in this study. One characterization method, by Cherubini and Peterson,[1] was a combination point and line count procedure developed for spherical UO_2 dispersed in stainless steel and fabricated at 1200°C. That method was developed to quantitatively evaluate fragmentation and stringering of the fuel. Unfortunately, it was not applicable to the present study. The aluminum-U_3O_8 dispersions fabricated at 500°C, under consideration in this study, contained highly fragmented and stringered particles, in contrast to the rounded unbroken UO_2 particles considered by Cherubini and Peterson.

Our purpose, therefore, was to find a suitable way to quantitatively evaluate fragmentation and stringering in the material under consideration and to propose a model that can be used to predict the fabrication behavior of similar fuel dispersions. In this preliminary study, we did not try to correlate the degree of fragmentation and stringering with the resulting irradiation performance. Such an evaluation is recommended because it should provide valuable information for selection of starting materials, evaluation of processing requirements, and estimation of overall fuel costs.

---

[1]J. H. Cherubini and S. Peterson, A Technique for the Quantitative Characterization of Dispersions, ORNL-TM-446 (Feb. 28, 1963).

DESCRIPTION OF MATERIALS

To obtain a variety of commercially available powders, we held the specifications for the U_3O_8 to a minimum. A high-fired grade of depleted U_3O_8 of particle size range −100 +325 mesh was specified. On this basis samples of commercial powder were obtained from three vendors. The as-received properties of the three oxides are listed in Table 1. The

Table 1. Properties of Commercial Powders of U_3O_8

Oxide	Sieve Cut	Analysis (%)	Density[a] (g/cm^3)	Surface Area[b] (m^2/g)	Uranium Analysis (%)
N	−80 +100	0.009	8.28	0.026	84.60
	−100 +140	21.9			
	−140 +200	33.9			
	−200 +270	21.8			
	−270 +325	15.2			
	−325	7.2			
S	−80 +100	0.19	8.26	0.058	84.72
	−100 +140	25.6			
	−140 +200	33.3			
	−200 +270	20.8			
	−270 +325	12.9			
	−325	7.2			
D	+100	0.005	8.28	0.107	82.89
	−100 +140	7.3			
	−140 +200	37.0			
	−200 +270	39.8			
	−270 +325	13.2			
	−325	2.7			

[a]Vacuum impregnation. Numbers rounded off from four decimal places.

[b]Static BET krypton adsorption.

oxides are identified by the letters N, S, and D to allow the vendors to remain anonymous. Figures 1, 2, and 3 show the three oxides in the as-received condition. Oxide N was made up of massive irregularly shaped particles containing reentrant surface cavities. The S oxide was cracked and very angular, almost acicular. The D oxide appeared to be composed of two different types of particles. One was irregularly rounded and often contained a few round holes; the other was spherical and somewhat porous.

Type X8001 aluminum powder, mesh size −100, was used as the matrix powder and type 6061 aluminum was used for the frames and cover plates. To promote bonding, the frames were alclad on two sides and the cover plates on one side with type 1100 aluminum.

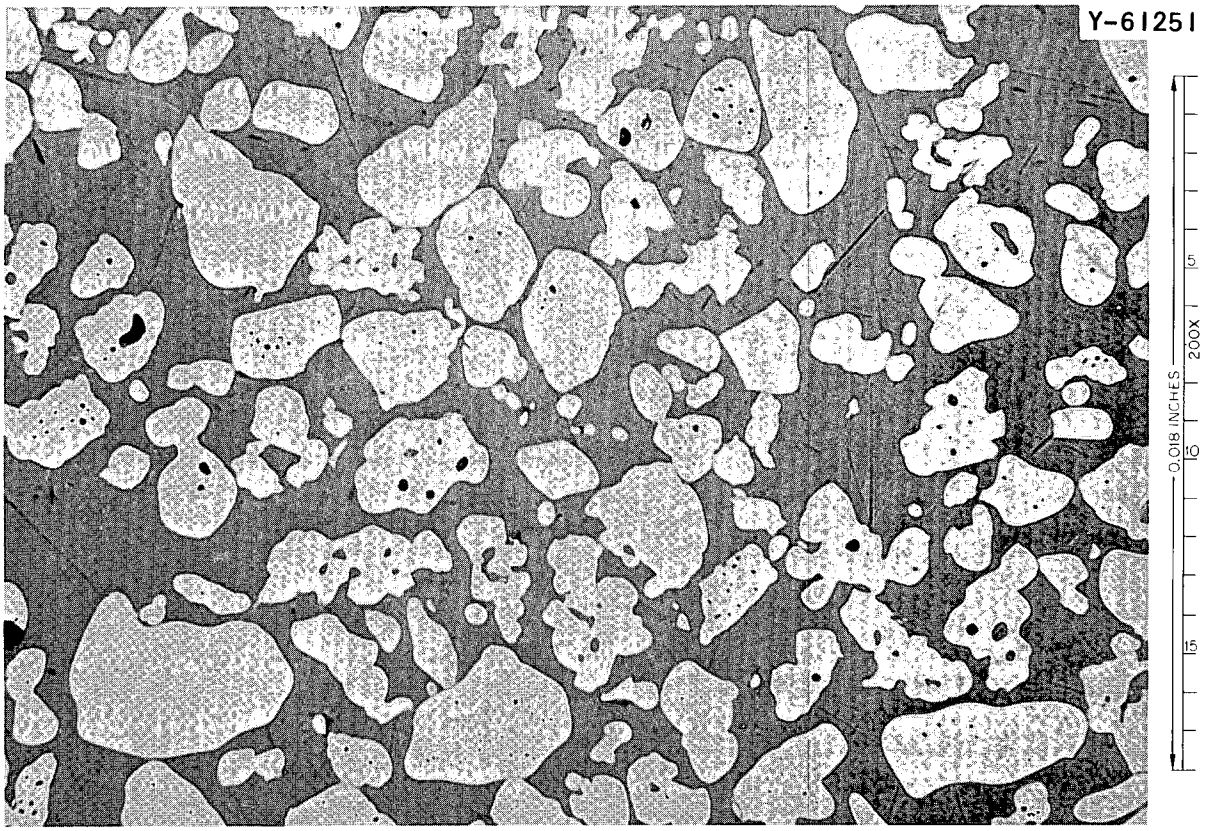

Fig. 1. As-Received Type N Oxide. Unetched.

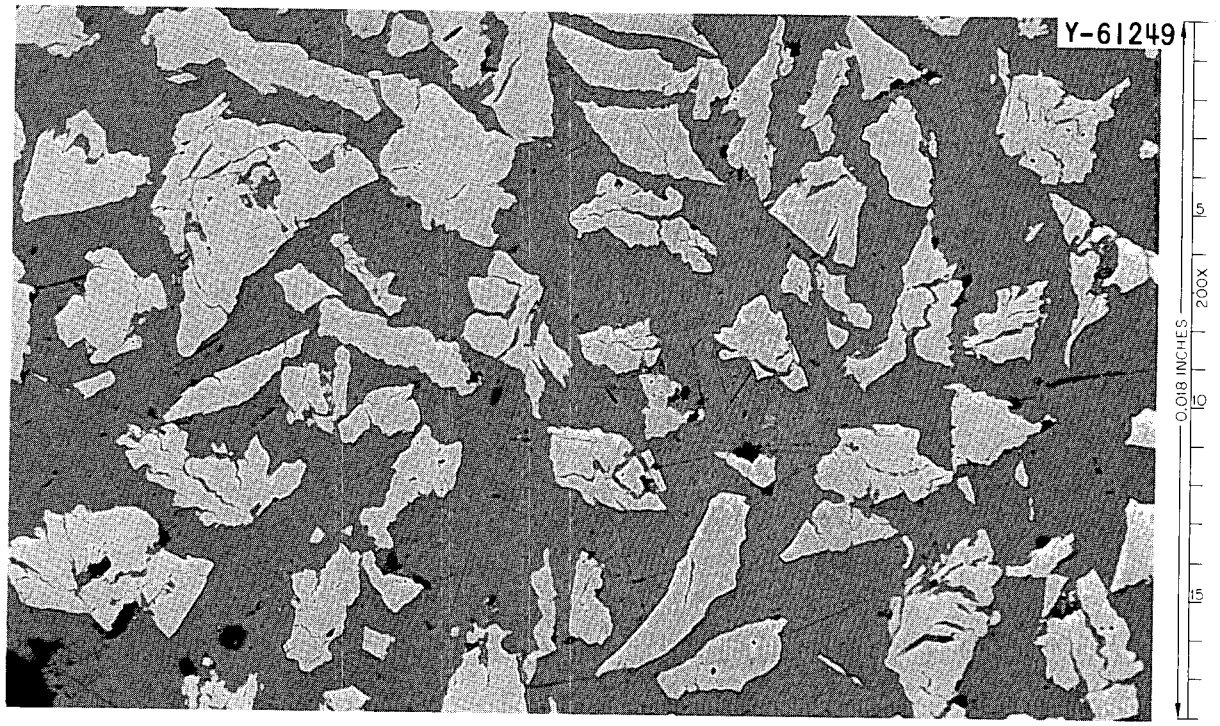

Fig. 2. As-Received Type S Oxide. Unetched.

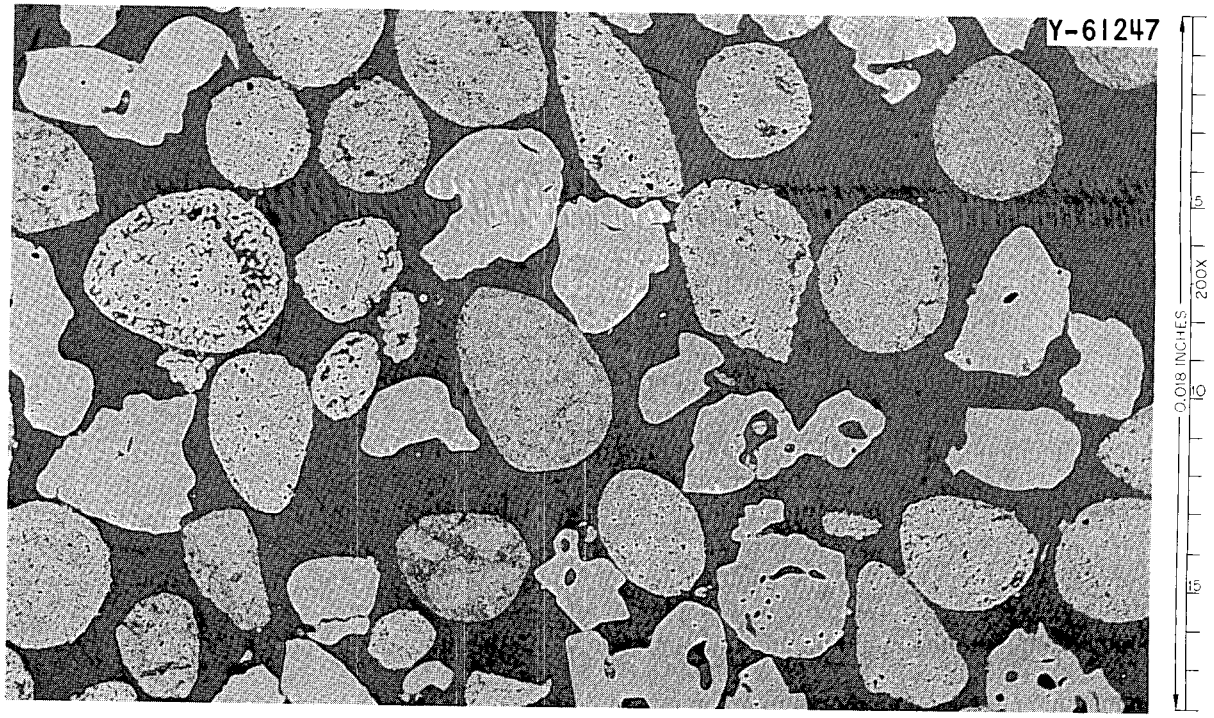

Fig. 3. As-Received Type D Oxide. Unetched.

EXPERIMENTAL PROCEDURES

Following previously developed ATR fabrication procedures,[2] each type oxide was weighed, mixed with type X8001 aluminum powder, blended, and pressed into fuel compacts. These fuel compacts were placed into type 6061 aluminum picture frames and enclosed in type 6061 aluminum cover plates, and the assembled billet was welded together. The billets were rolled to plates according to schedules listed in Table 2. Schedule A used only straight rolling. Schedule B, which included two passes of cross rolling, was identical with the schedule developed for plate 12 of the ATR fuel element.[2]

[2]D. O. Hobson, R. L. Heestand, and C. F. Leitten, Jr., Fabrication Development of U_3O_8-Aluminum Composite Fuel Plates for the Advanced Test Reactor, ORNL-3644 (July 1964).

Table 2. Rolling Schedules for Characterization Plates[a]

Schedule A		Schedule B	
Pass Number	Mill Setting	Pass Number	Mill Setting
1	0.494	1	0.494
2	0.395	2[b]	0.395
3	0.316	3[b]	0.336
4	0.253	4	0.286
5	0.202	5	0.229
6	0.162	6	0.183
7	0.130	7	0.146
8	0.104	8	0.118
9	0.083	9	0.094
10	0.066	10	0.075
11	0.058	11	0.066
12	0.054	12	0.058
		13	0.054
Cold rolled to 0.050 in.		Cold rolled to 0.050 in.	

[a]Starting billet thickness, 0.617 in. Hot rolling temperature, 500°C.

[b]Cross roll.

After being rolled, the plates were sectioned to provide metallographic samples: longitudinal samples from both ends and the center and a transverse sample from the center. The four samples from each plate were mounted together, polished, examined, and photographed. The center longitudinal section of each plate was photographed as a panorama; some 40 shots were made in groups of 10 each from 4 sections of each sample. This procedure yielded 24 strips of photographs; each strip represented approximately 1/4 in. of fuel length.

Since the fuel particles were highly fragmented, we wanted to use a counting method that did not depend upon line or point count methods or upon random counting methods for the determination of fragmentation. A very simple expedient was used; we counted every particle and every fragment in the 24 strips. This involved a total of 13,584 particles and 103,861 fragments. To do this we laid a clear plastic sheet over a photographic strip and, using a drawing pen (Rapidograph 00) with India ink, circled every original fuel particle. Then, each individual fragment within each circle was dotted with India ink. Following this, all of the circles and all of the fragments were counted. From the counts we obtained a fragmentation ratio by dividing the number of fragments by the number of original particles. Figure 4 shows portions of some of the plastic overlays.

A procedure such as this might lend itself to computer techniques. Just how is not readily apparent, however, since a human judgment factor is involved in deciding what was once an original particle and in resolving the very finely powdered fuel into individual fragments. Because of this factor, the marking and counting procedures were perforce limited to one individual who, to the best of his ability, strove to perform the procedures using the same rationale for all samples. Thus, the results are quantitative relative to each other whether they are absolute values or not. We believe that our values are very near the absolute values of fragmentation, since errors in judging particle identity are noncumulative. The most likely error in this procedure results from the inability to discriminate and count the very small fragments dispersed among the larger fragments.

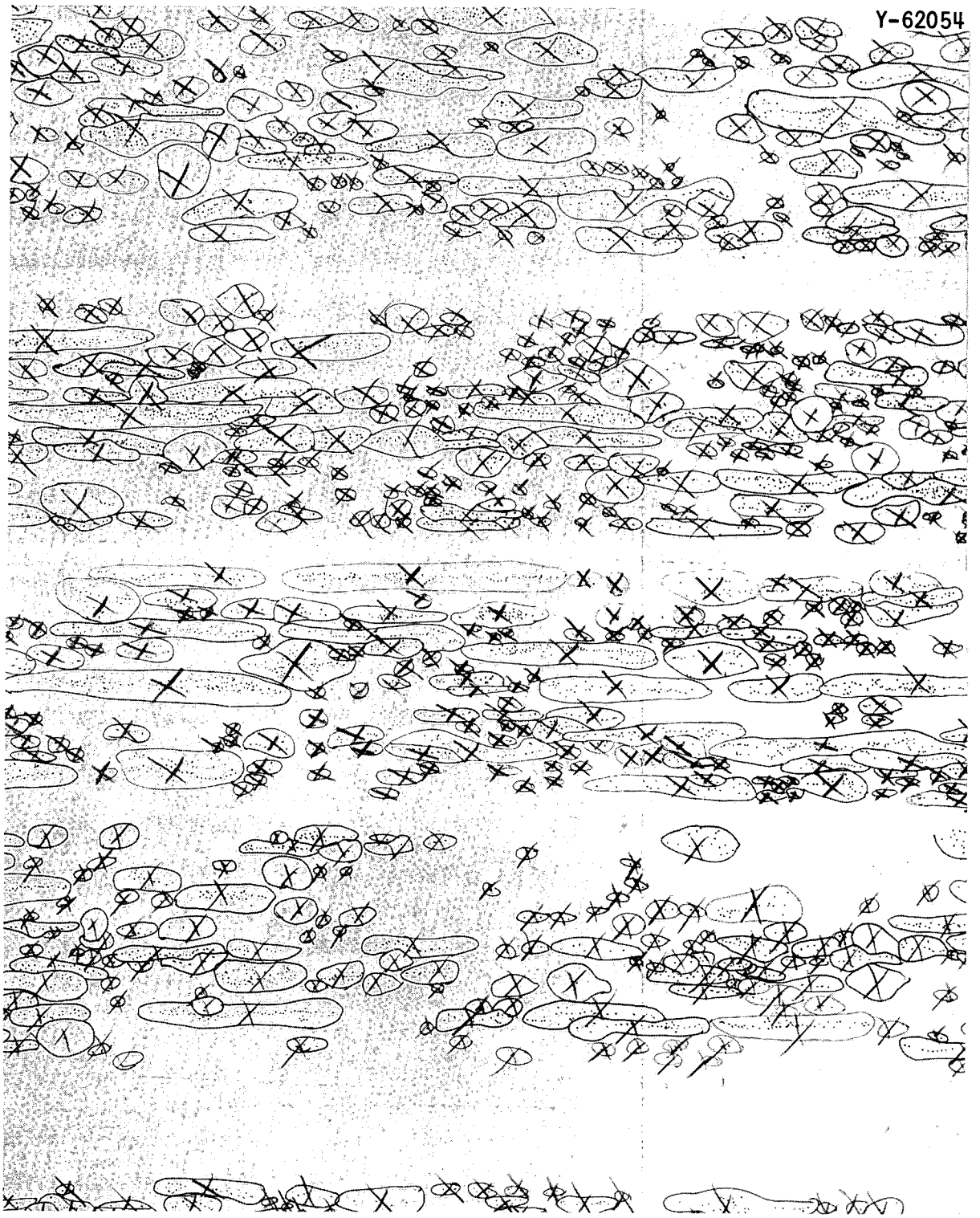

Fig. 4. Portions of Plastic Overlays Used to Index Rolled Plates. The closed curves encircle the particles judged to result from fragmentation of an original particle. The dots represent individual fragments. The cross marks indicate that the encircled marks have been tallied.

Good reproducibility was obtained in fragmentation determinations made on the D and N oxides. None varied more than ±10% from the average value for either oxide. The S oxide showed a much wider variation.

Cursory attempts were made to characterize the oxides on the basis of stringering, but the very highly stringered nature of the particles precluded any quantitative measurements. Stringering will be discussed qualitatively in a latter portion of the report.

RESULTS AND DISCUSSIONS

Our aim has been to quantitatively characterize the oxides and to prepare a model that could possibly be used to predict the fabrication behavior of the dispersoid in dispersion fuels. If successful, such data would be of valuable assistance in quantitatively assessing the irradiation performance of the fuel.

Quantitative data were obtained on the fragmentation behavior of three U_3O_8 oxide types dispersed in aluminum and fabricated by the two different rolling practices described in Table 2. The counting procedures yielded the fragmentation ratio values shown in Table 3 together with the data used to calculate the ratios.

The typical appearances of the types S, N, and D oxide dispersions in the photomicrographs used in obtaining the fragmentation ratios are shown in Figs. 5, 6, and 7, respectively. These microstructures were taken in the longitudinal direction of the fabricated plates for both rolling schedules. In both Figs. 6 and 7 the number of particle fragments appears greater in plates fabricated by cross-rolling schedules. This observation is in agreement with the fragmentation index ratios, although the value for the D-type oxide does not take into account the material contained in the fine stringered tails. This material, as shown in Fig. 7, was too finely divided to be resolved in the photographs and also was believed not to be a manifestation of fragmentation but, instead, fine material from the surface of the initial particles (see Fig. 3). Thus, the values for the D-type oxide represent a measure of the integrity of the bodies of the particles seen in the matrix and the material scoured from the particle surface.

Table 3. Experimental Fragmentation Data

Oxide, Rolling Schedule	View Number	Number of Original Particles	Number of Fragments	Fragmentation Index	Average
S, B	C-1-S (1)	870	5545	6.37	
	(11)	704	5443	7.73	7.54
	(21)	671	5066	7.55	
	(31)	838 (3083)	7200 (23,254)	8.59	
N, B	C-3-N (1)	600	5314	8.86	
	(11)	611	5289	8.66	8.70
	(21)	636	5677	8.93	
	(31)	600 (2447)	5023 (21,303)	8.37	
D, B	C-5-D (1)	468	2886	6.17	
	(11)	518	3277	6.33	
	(21)	557	3785	6.79	6.26
	(31)	458 (2001)	2579 (12,527)	5.67	
S, A	C-7-S (1)	622	5812	9.34	
	(11)	561	5746	10.24	
	(21)	556	5341	9.61	10.01
	(31)	482 (2221)	5328 (22,227)	11.05	
N, A	C-9-N (1)	450	3049	6.78	
	(11)	501	3384	6.75	
	(21)	508	3359	6.61	6.90
	(31)	554 (2013)	4092 (13,884)	7.39	
D, A	C-11-D (1)	491	2758	5.62	
	(11)	465	2561	5.51	
	(21)	352	2252	6.40	5.86
	(31)	511 (1819)	3095 (10,666)	6.06	

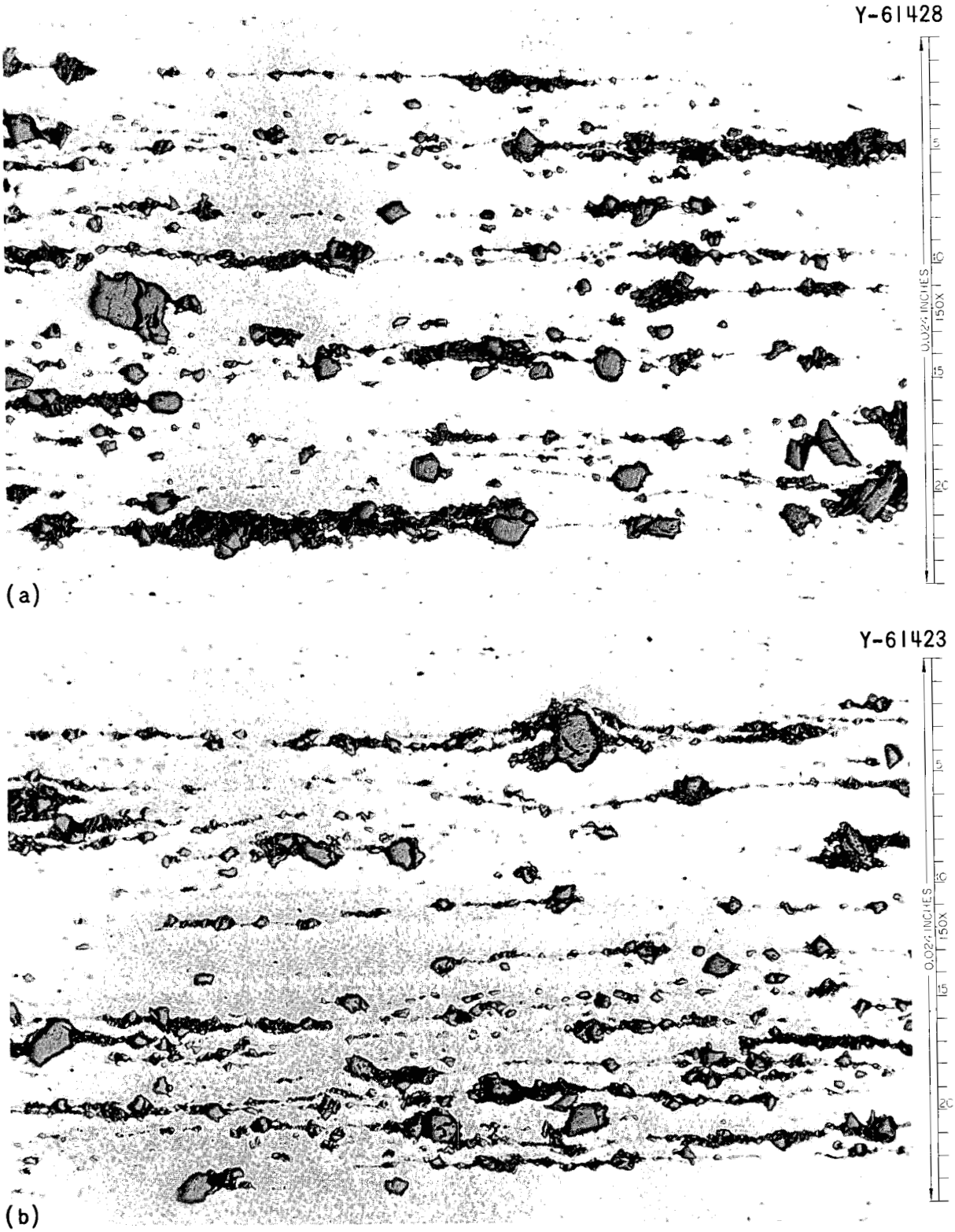

Fig. 5. Longitudinal Views of the S Oxide in Rolled Plates. Unetched. (a) Plate C-7-S, schedule A. (b) Plate C-1-S, schedule B.

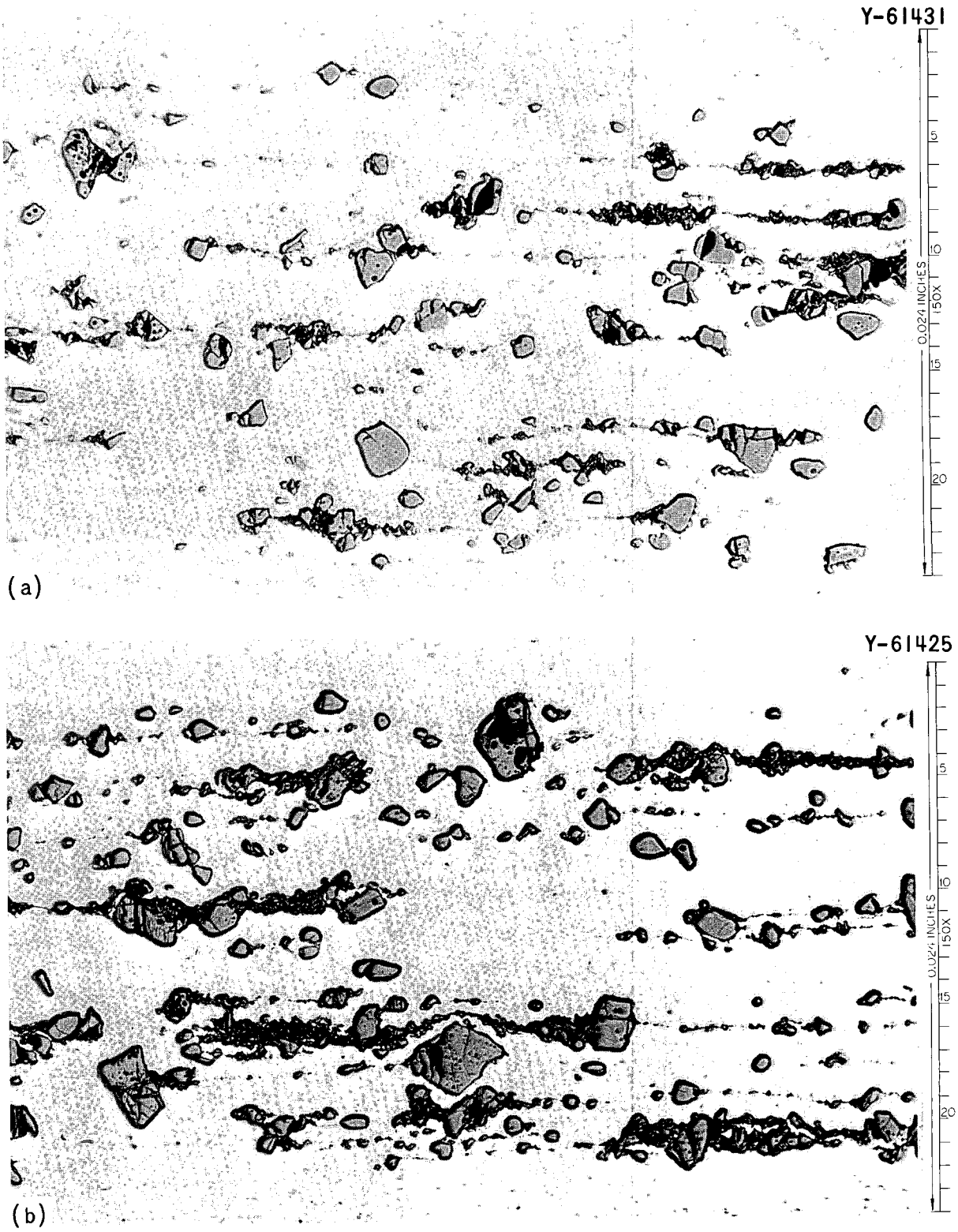

Fig. 6. Longitudinal Views of the N Oxide in Rolled Plates. Unetched. (a) Plate C-9-N, schedule A. (b) Plate C-3-N, schedule B.

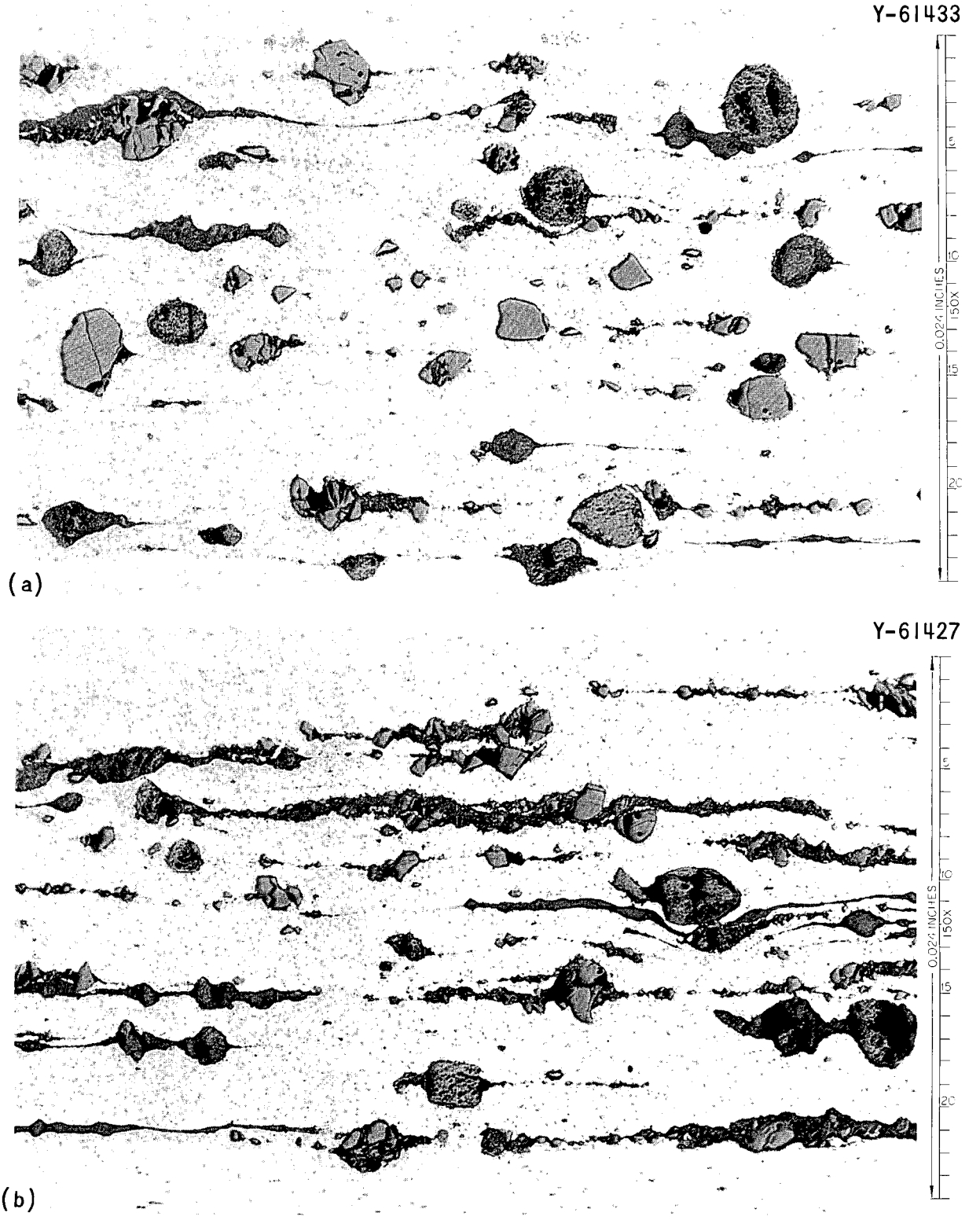

Fig. 7. Longitudinal Views of the D Oxide in Rolled Plates. Unetched. (a) Plate C-11-D, schedule A. (b) Plate C-5-D, schedule B.

The appearance of the S-type oxide, shown in Fig. 5, along with the corresponding fragmentation index ratio for the two rolling schedules deserves some explanation. The S-type oxide had the lowest density of the three oxides tested and generally appeared to fragment the most. The as-received powder, shown in Fig. 2, had cracks and an angular, almost acicular, shape. When the oxide was rolled according to schedule A (only straight rolling), each particle broke up into an average of 10 fragments. This requires little explanation. When the same oxide was rolled according to schedule B, however, the fragmentation ratio dropped to 7.5. This schedule includes a cross roll of 28% reduction in thickness, incorporated into the third and fourth passes. We believe that this cross rolling further elongated the very friable S particles in a direction normal to the straight-rolling direction and therefore out of the plane of polish of the metallographic specimen. In other words, the fragments were there but could not be seen. The contrast between Fig. 8, a transverse view of an exclusively straight-rolled plate containing S-type oxide and Fig. 9, a transverse view of a cross-rolled plate containing the same oxide, supports the contention. Significant stringering in this direction is seen only in the cross-rolled plate.

A correlation of the measured fragmentation index to the initial oxide particle properties was found to pose a somewhat subtle problem. Perhaps this difficulty would have been simplified if a greater variation in initial particle properties had been selected for this study.

Generally, the amount of fragmentation and subsequent stringering is related to the density of the oxide. Density, in the absence of complicating factors, is a direct indication of particle strength and integrity. This has been demonstrated for spheroidal UO_2 particles.[3] Particle shape can be an overriding factor, though, in causing particle breakup and stringering.

---

[3]A. J. Taylor, J. H. Cherubini, J. M. Robbins, and M. P. Haydon, Characterization of Spheroidal UO_2 Particles and Studies of Fabrication Variables for Core B Fuel Plates of the Enrico Fermi Fast Breeder Reactor, ORNL-3645 (August 1964).

Fig. 8. Transverse View of a Straight-Rolled (Schedule A) Plate Containing S Oxide.

Fig. 9. Transverse View of a Cross-Rolled (Schedule B) Plate Containing S Oxide.

As discussed previously, the D-type oxide had a low fragmentation ratio and had a high density (8.28 g/cm^3). According to metallographic evidence (Fig. 3), this oxide appears to be composed of two different types of particles. One was an irregularly rounded solid often containing a small number of round holes. The other was spherical and somewhat porous. The surface of this particle seems to have higher porosity than the center. Since this oxide had a high density measured with a vacuum impregnation technique, the porosity must be interconnected. The high surface area found for this oxide supports this contention. Examination of the as-rolled plate microstructure revealed that the outer layers of the spherical particles were stripped off during rolling. This produced an elongated tail extending from each particle in the rolling direction. These tails were composed of fines too small to be resolved in the microscope. When counting the fragments, we arbitrarily ignored the tails and classified them as surface fines that were scoured from the parent particles. This decision perhaps has biased the results to some extent. However, from a strict fragmentation standpoint, the correlation between density and particle integrity still stands.

The N-type oxide was different from the other two type oxides in that it was more sensitive to cross rolling. This oxide was made up of massive irregularly shaped particles containing reentrant surface cavities. We believe that this shape characteristic resulted in a greater susceptibility to fragmentation during a cross-rolling procedure than in a purely straight-rolling schedule. The particles developed a preferred orientation to each rolling direction. Hence, orientation direction changes twice during a schedule that calls for cross rolling. The S oxide on one hand was very brittle to start with and fragmented easily on the first pass. This rendered it insensitive to further fragmentation due to cross rolling *per se*. The N oxide, on the other hand, was apparently a strong oxide that was more resistant to fragmentation than the S oxide. When subjected to only straight rolling in schedule A, it was able to resist fragmentation to a high degree. Cross rolling, on the other hand, forced the particle to conform successively to the three different directions involved, and there was a far greater chance for particle breakdown.

We define stringering as the elongation of fragmented oxide particles in the rolling direction. In going through the counting procedure on the characterization plates, we observed a rather elementary truth: depending upon where in the rolling schedule the particles started to fragment, their elongation or stringering was due to the remainder of the rolling schedule.

The relative life of a coherent fuel particle directly determines the relative degree of stringering that occurs during rolling. This is shown in Fig. 10, which is an idealized illustration of this effect. In this illustration, four similar particles are assumed to undergo identical rolling treatments. The first particle is postulated to fracture on the first pass, the second on the second pass, the third on the fifth pass, and the fourth on the seventh pass. By the tenth pass, as a result of repeated fragmentation, the particles are vastly dissimilar in length, with the first particle to fragment being the longest. This is a very elementary concept, but it is important because it relates stringering directly to particle strength.

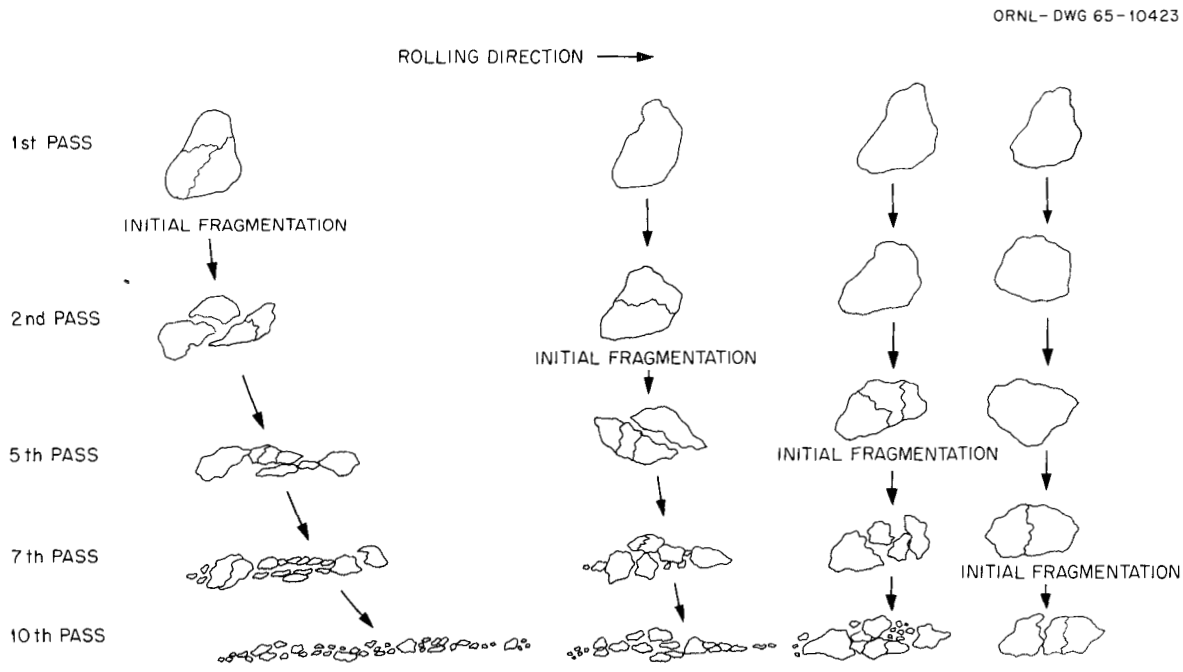

Fig. 10. Idealized Representation of the Relationship Between Particle Life and Stringering.

At the plate fabrication temperature of 500°C the fuel particles suffer little, if any, plastic deformation. Therefore, all elongation is effected by the plastic flow of the aluminum matrix. Any loss of integrity by the particles is magnified by the elongating action of the plastic aluminum.

We postulate that stringer length decreases with increasing particle life. Also, particle life increases with inherent particle density, rolling temperature, particle sphericity, and particle spacing and decreases with surface area. The number of surviving particles decreases with the total number of rolling passes. We also postulate that particle life depends on the amount of reduction per pass, the amount of fuel in the core, and the amount of cross roll. The exact interrelationships among these variables would be difficult at present to guess and were not evaluated in this study.

From measurements of stringer length and from a knowledge of particle size distribution, one should be able to arrive at a value for the average particle life. Unfortunately, however, one cannot directly measure the length of fuel particles from a two-dimensional photograph. As discussed in the literature,[4] a statistical approximation of the volume fraction of a constituent dispersed in an alloy may be calculated from either areal or lineal analysis. However, we have no simple way to measure the geometry of particles of a constituent embedded in an opaque medium. Or more practically, we cannot measure the envelope of a particle as it fragments. We postulate that as a particle fragments during rolling, it is contained within a flattened envelope, as shown in Fig. 11. The figure clearly shows that a specimen mounted and polished to show a longitudinal view would seldom, if ever, show the true length of the particle. By successive grinding and polishing of the mounted specimen, one might determine the stringer lengths in a volume of matrix and from this arrive at a value for the average particle life, but the effort expended in

---

[4]J. E. Hilliard, Volume-Fraction Analysis by Quantitative Metallography, Rept. No. 61-RL-2652M, G.E. Research Laboratory (March 1961).

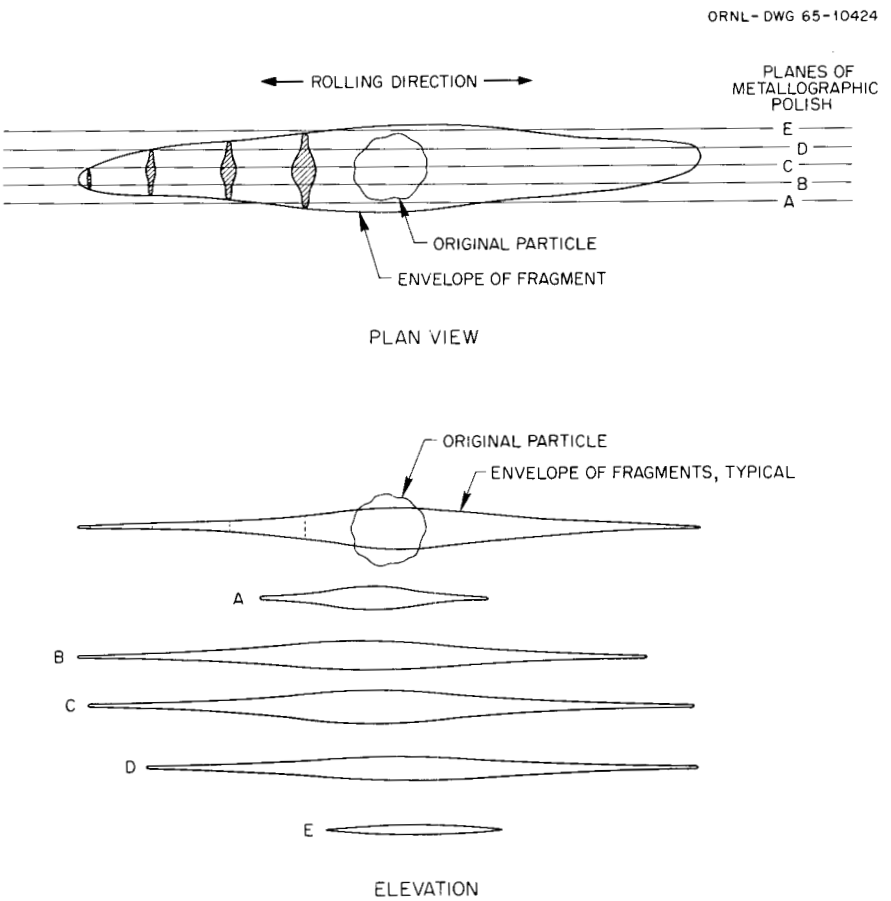

Fig. 11. Idealized Representation of the Distribution of Fragments and Its Effect on Metallographic Examination.

proving a rather apparent truth might not be worthwhile. Thus, we believe that stringer length is related to particle life, but we do not have the means for showing the quantitative relationship.

CONCLUSIONS

The exploratory nature of this work excludes drawing firm conclusions. Our purpose was to establish a suitable way to quantitatively evaluate fragmentation and stringering in dispersion plates containing irregular as well as spherical oxide particles. No attempt was made to correlate our finding with the subsequent irradiation performance of the fuel, although such a correlation would be beneficial in evaluating fuel processing requirements and possible fuel cost reductions.

In general, we found that fragmentation experienced by oxide particles during plate processing could result from lack of apparent strength as reflected by density and microstructure and to sometimes overriding factors of particle shape. Although not conclusively shown, the fabrication behavior of oxide particles can possibly be predicted from the physical properties of the oxide and the particle shape.

The method used to determine the fragmentation index appears valid for characterizing the quality of the dispersion with respect to initial oxide properties. As in the case of dispersions of spherical oxide, particles with a low initial density were more prone to fragmentation.

Although we were unable to quantitatively evaluate fuel particle stringering, the degree of stringering appeared to be associated with the rate of particle fragmentation. Particles which fragmented during initial rolling passes exhibited a larger degree of stringering. Similarly, oxides with large surface areas were also more prone to surface particle scouring and the subsequent stringering of the fine particles.

ACKNOWLEDGMENT

The authors are indebted to J. N. Hix and C. W. Holland for rolling the plates used in this study, to W. R. Laing for the chemical analyses, to the Metallography Group for the photomicrographs, and to the Graphic Arts Section for the drawings.

Thanks are extended to the Metals and Ceramics Division Reports Office and to Sigfred Peterson for help in preparation of this report.

ORNL-TM-1692

INTERNAL DISTRIBUTION

1–3. Central Research Library
4–5. ORNL – Y-12 Technical Library Document Reference Section
6–35. Laboratory Records
36. Laboratory Records, ORNL R.C.
37. ORNL Patent Office
38. G. M. Adamson, Jr.
39. J. H. Barrett
40. S. E. Beall
41. R. J. Beaver
42. M. Bender
43. R. G. Berggren
44. D. S. Billington
45. A. L. Boch
46. B. S. Borie
47. G. E. Boyd
48. W. H. Bridges
49. R. B. Briggs
50. W. E. Brundage
51. R. M. Carroll
52. J. H. Crawford
53. J. E. Cunningham
54. J. H. DeVan
55. A. P. Fraas
56. J. H Frye, Jr.
57. R. J. Gray
58. W. R. Grimes
59. W. O. Harms
60–62. M. R. Hill
63. N. E. Hinkle
64–89. D. O. Hobson
90. H. W. Hoffman
91. W. R. Huntley
92. H. Inouye
93. G. W. Keilholtz
94. B. C. Kelley
95. J. A. Lane
96. C. F. Leitten, Jr.
97. A. P. Litman
98. A. L. Lotts
99. R. N. Lyon
100. H. G. MacPherson
101. R. E. MacPherson
102. W. R. Martin
103. R. W. McClung
104. H. E. McCoy, Jr.
105. H. C. McCurdy
106. D. L. McElroy
107. C. J. McHargue
108. F. R. McQuilkin
109. A. J. Miller
110. E. C. Miller
111. J. G. Morgan
112. F. H. Neill
113. S. M. Ohr
114. P. Patriarca
115. A. M. Perry
116. S. Peterson
117. R. E. Reed
118. P. L. Rittenhouse
119. W. C. Robinson
120. M. W. Rosenthal
121. G. Samuels
122. J. L. Scott
123. O. Sisman
124. G. M. Slaughter
125. N. K. Smith
126. I. Spiewak
127. J. T. Stanley
128. W. J. Stelzman
129. J. O. Stiegler
130. D. B. Trauger
131. R. P. Tucker
132. G. M. Watson
133. A. M. Weinberg
134. J. R. Weir, Jr.
135. G. D. Whitman
136. F. W. Young, Jr.

EXTERNAL DISTRIBUTION

137–138. F. W. Albaugh, Battelle, PNL
139. R. J. Allio, Westinghouse Atomic Power Division
140. R. D. Baker, Los Alamos Scientific Laboratory
141. C. Baroch, Babcock and Wilcox
142. L. Brewer, University of California, Berkeley

143. V. P. Calkins, GE, NMPO
144. W. Cashin, Knolls Atomic Power Laboratory
145. S. Christopher, Combustion Engineering, Inc.
146. D. B. Coburn, General Atomic
147. D. F. Cope, RDT, OSR, AEC, Oak Ridge National Laboratory
148. G. K. Dicker, Division of Reactor Development and Technology, AEC, Washington
149. D. E. Erb, Division of Reactor Development and Technology, AEC, Washington
150. E. A. Evans, GE, Vallecitos
151. W. C. Francis, Idaho Nuclear Corporation
152. A. J. Goodjohn, General Atomic
153. R. G. Grove, Mound Laboratory
154. D. H. Gurinsky, BNL
155. A. N. Holden, GE, APED
156–158. J. S. Kane, Lawrence Radiation Laboratory, Livermore
159. H. Kato, U.S. Department of the Interior, Bureau of Mines
160. J. H. Kittel, ANL
161. E. J. Kreih, Westinghouse, Bettis Atomic Power Laboratory
162. W. J. Larkin, AEC, Oak Ridge Operations
163. W. L. Larsen, Iowa State University, Ames Laboratory
164. J. J. Lombardo, NASA, Lewis Research Center
165. J. H. MacMillan, Babcock and Wilcox Company
166. R. Mayfield, ANL
167. M. McGurty, GE, NMPO
168. M. Nevitt, ANL
169. R. E. Pahler, Division of Reactor Development and Technology, AEC, Washington
170. S. Paprocki, BMI
171. D. Ragone, General Atomic
172. B. Rubin, Lawrence Radiation Laboratory, Livermore
173. F. C. Schwenk, Division of Reactor Development and Technology, AEC, Washington
174–176. J. M. Simmons, Division of Reactor Development and Technology, AEC, Washington
177. L. E. Steele, Naval Research Laboratory
178. R. H. Steele, Division of Reactor Development and Technology, AEC, Washington
179. W. F. Sheely, Division of Research, AEC, Washington
180. A. Strasser, United Nuclear Corporation
181. A. Taboada, Division of Reactor Development and Technology, AEC, Washington
182. A. Van Echo, Division of Reactor Development and Technology, AEC, Washington
183. R. Van Tyne, Illinois Institute of Technology Research Institute
184. C. E. Weber, Atomics International
185. G. W. Wensch, Division of Reactor Development and Technology, AEC, Washington
186. Division of Research and Development, AEC, Oak Ridge Operations
187–201. Division of Technical Information Extension